



Structural basis for hijacking of the host ACBD3 protein by bovine and porcine enteroviruses and kobuviruses

Miroslav Smola¹ · Vladimira Horova¹ · Evzen Boura¹ · Martin Klima¹

Received: 6 August 2019 / Accepted: 31 October 2019 / Published online: 16 December 2019
© Springer-Verlag GmbH Austria, part of Springer Nature 2019

Abstract

Picornaviruses infect a wide range of mammals including livestock such as cattle and swine. As with other picornavirus genera such as *Aphthovirus*, there is emerging evidence of a significant economic impact of livestock infections caused by members of the genera *Enterovirus* and *Kobuvirus*. While the human-infecting enteroviruses and kobuviruses have been intensively studied during the past decades in great detail, research on livestock-infecting viruses has been mostly limited to the genomic characterization of the viral strains identified worldwide. Here, we extend our previous studies of the structure and function of the complexes composed of the non-structural 3A proteins of human-infecting enteroviruses and kobuviruses and the host ACBD3 protein and present a structural and functional characterization of the complexes of the following livestock-infecting picornaviruses: bovine enteroviruses EV-E and EV-F, porcine enterovirus EV-G, and porcine kobuvirus AiV-C. We present a series of crystal structures of these complexes and demonstrate the role of these complexes in facilitation of viral replication.

Introduction

Enteroviruses and kobuviruses are small non-enveloped positive-sense single-stranded RNA viruses that belong to the family *Picornaviridae* of the order *Picornavirales*. They can infect a wide range of mammals including humans and livestock such as cattle and swine. Currently, the genus *Enterovirus* consists of 15 species, *Enterovirus A-L* and *Rhinovirus A-C*, while the genus *Kobuvirus* consists of six species, *Aichivirus A-F* [1]. In this study, we focus on the livestock-infecting enteroviruses and kobuviruses, namely two bovine enteroviruses, enterovirus E (EV-E) and enterovirus F (EV-F), the porcine enterovirus EV-G, and porcine kobuvirus aichivirus C (AiV-C).

The bovine enteroviruses EV-E and EV-F are endemic in cattle populations worldwide. They have been isolated from cattle with a wide range of clinical signs including gastrointestinal and respiratory diseases, reproductive disorders, and infertility [2–4]. The porcine enterovirus EV-G has been isolated from swine faecal samples in Europe, Asia, and North America, as well as from wild boars. Their infections may be asymptomatic; however, an association with diarrhoea, dermal lesions, pyrexia, or flaccid paralysis has occasionally been observed [5–7]. The porcine kobuvirus AiV-C has been reported in several European, Asian, and American countries among domestic pigs and wild boars [8, 9]. Infections with this virus have been reported to correlate with diarrhoea in pigs [10].

Enterovirus and kobuvirus genomes are approximately 7.4 kb and 8.3 kb in length, respectively, and encode single polyproteins. Their open reading frames are flanked by 5' and 3' untranslated regions (5'- and 3'-UTRs). The 5'-UTR contains a cloverleaf-like structure that is indispensable for viral replication and an internal ribosome entry site that is crucial for viral cap-independent translation. After translation, viral polyproteins are cleaved by viral proteases, generating both structural (VP1–VP4) and non-structural (2A–2C and 3A–3D) proteins. In addition, kobuviruses encode a leader protein (L^{PRO}), which is located at the N-terminus of the kobuviral polyprotein but is absent in enteroviruses. In

Handling Editor: Diego G. Diel.

Miroslav Smola and Vladimira Horova contributed equally.

✉ Evzen Boura
boura@uochb.cas.cz

✉ Martin Klima
klima@uochb.cas.cz

¹ Institute of Organic Chemistry and Biochemistry, Czech Academy of Sciences, Prague, Czech Republic

this study, we focus on the small non-structural 3A protein, which is a critical component of the viral replication complex and is responsible for the recruitment of one or more host factors to the site of viral replication.

Acyl-CoA-binding domain-containing protein-3 (ACBD3) is a well-described host protein that is recruited to the viral replication site by a direct protein-protein interaction with the viral 3A protein. It is a multifunctional, multidomain, Golgi-resident protein [11] that facilitates replication of all enteroviruses and kobuviruses studied so far [12–18]. The interaction between the viral 3A protein and the host ACBD3 protein is mediated by the N-terminal cytoplasmic domain of the 3A protein and the C-terminal Golgi-dynamics domain (GOLD) of ACBD3. In our recent studies, we analyzed the structure and function of the complexes composed of the ACBD3 GOLD domain and the 3A proteins of enteroviruses EV-A to EV-D and kobuviruses AiV-A and AiV-B [19, 20]. Here, we extend our previous work to the analysis of the complexes formed by the GOLD domain of bovine and porcine ACBD3 and the bovine and porcine enteroviruses EV-E to EV-G and the porcine kobuvirus AiV-C.

Materials and methods

Plasmids

A human ACBD3-encoding plasmid was kindly provided by Carolyn Machamer. To generate plasmids encoding the bovine and porcine ACBD3 GOLD domains (corresponding to GenBank accession numbers NP_001178112.1 and NP_001009581.1, respectively), the human ACBD3-encoding plasmid was used as a template. Mutations corresponding to the respective substitutions of the amino acid residues were introduced by site-directed mutagenesis using Phusion Flash High-Fidelity PCR Master Mix (Thermo Scientific). For expression in *Escherichia coli*, the bovine and porcine ACBD3 GOLD-domain-encoding regions were cloned into a pRSFD vector (Novagen) with an N-terminal 6xHis tag followed by a GB1 solubility tag and a TEV protease cleavage site using PCR and restriction endonuclease recognition site cloning. For bacterial expression of the EGFP-GOLD fusion proteins, the EGFP-encoding sequence was inserted between the TEV cleavage site and the GOLD-domain-encoding regions.

The genomes of enterovirus F2 (corresponding to GenBank accession no. DQ092795) and enterovirus G1 (corresponding to GenBank accession no. AF363453) lacking the capsid-protein-encoding regions were generated synthetically by GeneArt synthesis (Thermo Scientific). The pT7-EVF2/mCherry and pT7-EVG1/mCherry plasmids for viral subgenomic replicon assays were generated by subcloning

these synthetically constructed genes under the control of a T7 promoter and inserting the gene encoding the mCherry fluorescent protein [21] at the position of the capsid-protein-encoding region by Gibson assembly [22]. Mutations were generated by site-directed mutagenesis using Phusion Flash High-Fidelity PCR Master Mix (Thermo Scientific). For expression of the EGFP-fused full-length 3A protein of enterovirus F2 and its mutants in mammalian cells, the respective wild-type and mutant 3A-protein-encoding genes were recloned into the pEGFP-C1 vector (Clontech) using PCR and restriction endonuclease recognition site cloning.

For bacterial expression of the cytoplasmic domains of various enteroviral and kobuviral 3A proteins, the respective 3A-protein-encoding genes were generated directly from synthetic oligonucleotides (Sigma) by PCR and subcloned into the pRSFD vector (Novagen) with an N-terminal 6xHis tag followed by a GB1 solubility tag and a TEV protease cleavage site using PCR and restriction endonuclease recognition site cloning. For bacterial expression of the GOLD/3A complexes used for the crystallographic experiments, the respective ACBD3 GOLD-domain-encoding regions were subcloned into the second multiple cloning site of this plasmid using PCR and restriction endonuclease recognition site cloning.

All DNA constructs were verified by sequencing.

Protein expression and purification

All recombinant proteins used in this study were bacterially expressed as fusion proteins with an N-terminal 6x histidine (His_6) purification tag followed by a GB1 solubility tag and a TEV protease cleavage site. For the structural analysis of the GOLD/3A complexes, the cytoplasmic domains of the 3A proteins, which were N-terminally fused to His_6 -GB1-TEV were directly co-expressed with the untagged ACBD3 GOLD domains. The proteins were expressed in the *E. coli* BL21 DE3 NiCo bacterial strain (New England Biolabs) in autoinduction ZY medium. Bacterial cells were harvested by centrifugation at 5,000 g for 8 min and lysed using a French press cell disruptor instrument (Thermo) at 1,000 psi in lysis buffer (50 mM Tris-HCl, pH 8, 300 mM NaCl, 3 mM β -mercaptoethanol, 30 mM imidazole, and 10% glycerol). The lysate was incubated with HisPur Ni-NTA Superflow agarose (Thermo Fisher Scientific) for 30 min, and the agarose beads were then extensively washed with wash buffer (50 mM Tris-HCl pH 8, 300 mM NaCl, 1 mM β -mercaptoethanol, and 20 mM imidazole). The proteins of interest were eluted with elution buffer (50 mM Tris-HCl, pH 8, 200 mM NaCl, 3 mM β -mercaptoethanol, and 300 mM imidazole).

For biochemical analysis of the 3A proteins by micro-scale thermophoresis, the N-terminal His_6 -GB1 tags were preserved to increase protein solubility and to avoid

aggregation at the required concentrations. For the crystallographic analysis of the GOLD/3A complexes, the N-terminal His₆-GB1 tags were removed using TEV protease. Next, the proteins were purified using size-exclusion chromatography on a HiLoad 16/60 Superdex 75 prep grade column (GE Healthcare) in storage buffer (10 mM Tris-HCl, pH 8, 200 mM NaCl, and 3 mM β-mercaptoethanol). In addition, the GOLD/3A complexes used for the crystallographic analysis were further purified by reverse immobilized metal affinity chromatography, using a HisTrap HP column (GE Healthcare), while the EGFP-fused ACBD3 GOLD domains used for microscale thermophoresis were further purified using ion exchange chromatography on a MonoQ 10/100 GL column (GE Healthcare) and then dialyzed overnight against the storage buffer.

The molecular weight and purity of all proteins was verified by SDS-PAGE and matrix-assisted laser desorption/ionisation (MALDI) analysis [23]. Purified proteins were concentrated to 1–10 mg/ml, aliquoted, flash frozen in liquid nitrogen, and stored at -80 °C until needed.

Crystallization and crystallographic analysis

Protein crystals were obtained at 291 K in sitting drops, using the vapor diffusion method. They were cryoprotected, flash frozen in liquid nitrogen, and analyzed by X-ray crystallography. The datasets were collected from single frozen crystals at the MX14.1 beamline of the synchrotron BESSY II at Helmholtz-Zentrum Berlin [24]. Data were integrated and scaled using XDS [25] and XDSAPP [26]. Structures were determined by molecular replacement using the unliganded human ACBD3 GOLD domain structure (pdb code 5LZ1) as a search model. The initial models were obtained with Phaser [27] from the Phenix package [28]. The models were further improved using automatic model building with Buccaneer [29] from the CCP4 suite [30], automatic model refinement with Phenix.refine [31] from the Phenix package [28], and manual model building with Coot [32]. Statistics for data collection and processing and structure determination and refinement are summarized in Table 1. Structural figures were generated with PyMol [33]. The

Table 1 Statistics for data collection and processing, structure solution and refinement of the porcine kobuvirus AiV-C 3A protein in complex with the porcine ACBD3 GOLD domain (*Ss* GOLD+AiV-C 3A), the bovine enterovirus EV-F2 3A protein fused to the bovine ACBD3 GOLD domain (*Bt* GOLD+EV-F2 3A), and

the porcine enterovirus EV-G1 3A protein in complex with the porcine ACBD3 GOLD domain (*Ss* GOLD+EV-G1 3A). Numbers in parentheses refer to the highest resolution shell of the respective dataset. r.m.s.d., root-mean-square deviation

Crystal	<i>Ss</i> GOLD + AiV-C 3A	<i>Bt</i> GOLD + EV-F2 3A	<i>Ss</i> GOLD + EV-G1 3A
Construct	wild type	fusion protein	wild type
PDB accession code	6Q67	6Q68	6Q69
Data collection and processing			
Space group	P 31 2 1	P 43	P 1
Cell dimensions - a, b, c (Å)	55.4 55.4 169.5	55.37 55.37 200.86	54.85 55.77 61.16
Cell dimensions - α, β, γ (°)	90.0 90.0 120.0	90.0 90.0 90.0	96.2 105.5 112.8
Resolution at I/σ(I) = 2 (Å)	2.42	3.27	2.85
Resolution range (Å)	47.97 - 2.25 (2.328 - 2.25)	48.49 - 3.16 (3.27 - 3.16)	30.16 - 2.75 (2.85 - 2.75)
No. of unique reflections	14,951 (1,448)	10,318 (1,049)	14,434 (1,306)
Completeness (%)	99.07 (97.57)	99.78 (99.24)	88.55 (80.62)
Multiplicity	5.8 (6.1)	7.5 (7.3)	2.1 (2.1)
Mean I/σ(I)	21.49 (1.01)	16.06 (1.47)	8.37 (1.38)
Wilson B factor (Å ²)	68.26	114.03	56.41
R-merge / R-meas (%)	3.61 / 3.99	7.81 / 8.40	8.09 / 10.92
CC1/2	1.000 (0.799)	0.999 (0.662)	0.997 (0.720)
CC*	1.000 (0.942)	1.000 (0.892)	0.999 (0.915)
Structure solution and refinement			
R-work (%)	23.44 (39.50)	24.34 (33.35)	23.13 (38.20)
R-free (%)	26.80 (42.56)	27.85 (35.60)	27.21 (46.31)
R.m.s.d. - bonds (Å) / angles (°)	0.008 / 1.14	0.003 / 0.77	0.003 / 0.81
Average B factors (Å ²)	79.0	112.9	71.8
Clashscore	0.00	2.65	0.55
Ramachandran favored/outliers (%)	100 / 0	96 / 0	98 / 0

atomic coordinates and structural factors were deposited in the Protein Data Bank (<https://www.rcsb.org>).

Microscale thermophoresis (MST)

Microscale thermophoresis was performed using a Monolith NT.115 instrument (NanoTemper Technologies) according to the manufacturer's instructions. Monolith NT.115 standard treated capillaries were loaded with a mixture of the EGFP-fused bovine or porcine ACBD3 GOLD domain at a constant concentration of 150 nM in MST buffer (30 mM Tris-HCl, pH 7.4, 150 mM NaCl, and 3 mM β -mercaptoethanol) and the GB1-fused viral 3A protein in a series of concentrations ranging from 20 nM to 10 μ M. Temperature-dependent changes in fluorescence and the thermophoretic motion of the fluorescent protein were analyzed using Monolith NT Analysis Software.

Calculation of interaction energies

Rapid calculations of changes in ACBD3/3A interaction energies of various to-alanine mutants of the GOLD/3A complexes were carried out using the Pssm tool of the FoldX software package [34], using the atomic coordinates from the respective crystal structures.

Tissue cultures and transfections

Bovine kidney cells MDBK (Leibniz-Institute DSMZ #ACC 174), porcine kidney cells PK-15 (Leibniz-Institute DSMZ #ACC 640), and human embryonic kidney cells HEK293T (ATCC) were maintained in Dulbecco's modified Eagle's medium (Sigma) supplemented with 10% fetal calf serum (Gibco). Transfection of MDBK and PK-15 cells with viral subgenomic RNA was performed using a TransIT mRNA Transfection Kit (Mirus Bio). Transfection of HEK293T cells with plasmid DNA was performed using polyethyl-eneimine (Sigma).

Co-immunoprecipitation assay

HEK293T cells were transfected with the appropriate mutants of the EGFP-fused 3A protein of enterovirus F2. The next day, cells were harvested, washed twice with phosphate-buffered saline (PBS) and lysed in ice-cold lysis buffer (20 mM Tris-HCl, pH 7.4, 100 mM NaCl, 50 mM NaF, 10 mM EDTA, 10% glycerol, and 1% NP-40) supplemented with protease inhibitors (cOmplete Protease Inhibitor Cocktail, Sigma/Roche). After solubilization for 15 min on ice, the lysate was precleared by centrifugation at 16,000 g for 15 min. The resulting supernatant was incubated with GFP-nanobody-coupled Sepharose beads (GFP-Trap, ChromoTek) for 1 h at 4 °C. After three washes with 10 volumes of the

lysis buffer, the bound proteins were eluted directly with Laemmli sample buffer, subjected to SDS-PAGE, and analyzed by immunoblotting. The whole-cell lysates and eluted proteins were stained with mouse monoclonal antibodies to GFP (Santa Cruz Biotechnology, sc-9996), ACBD3 (Santa Cruz Biotechnology, sc-101277), and GBF1 (Santa Cruz Biotechnology, sc-136240). Images were acquired using an LI-COR Odyssey Infrared Imaging System.

Virus subgenomic replicon assay

The pT7-EVF2/mCherry and pT7-EVG1/mCherry wild-type and mutant plasmids were linearized by cleavage with HindIII-HF (Thermo Fisher Scientific) and purified using mini spin columns (Epoch Life Science). Viral subgenomic replicon RNA was generated using a TranscriptAid T7 High Yield Transcription Kit (Thermo Fisher Scientific) and purified using RNeasy mini spin columns (QIAGEN). For replicon assays, bovine MDBK and porcine PK-15 cells grown in 24-well plates were transfected with the T7-amplified RNA using a TransIT mRNA transfection kit (Mirus Bio). At various time points from 4 to 10 hours post-transfection, the cells were harvested by trypsinization and stained with Hoechst33258 dye to determine cell viability utilizing the increased efflux of this dye from live cells. Cell fluorescence was then determined by flow cytometry using a BD LSR Fortessa cell analyzer (BD Biosciences) and the following optical configurations: mCherry: 561 nm laser, 670/30 nm bandpass filter; Hoechst33258: 405 nm laser, 450/50 nm bandpass filter. The data were analyzed using FlowJo software. The mean fluorescence intensity of the reporter mCherry, calculated from all singlet cells, and the percentage of cells with mCherry fluorescence intensity above background were determined to quantify the level of RNA replication.

Results

Bovine and porcine enterovirus 3A proteins interact with the host ACBD3 protein *in vitro* with dissociation constants in the submicromolar range

In a previous study [19], we determined the dissociation constants of the complexes composed of the host ACBD3 protein and the 3A proteins of several kobuviruses, including bovine kobuvirus ($K_D \sim 8 \mu$ M) and porcine kobuvirus ($K_D \sim 4 \mu$ M). In this study, we aimed to determine the strength of the interaction between the host ACBD3 proteins and the 3A proteins of several representative bovine and porcine enteroviruses. For that purpose, we expressed the cytoplasmic domains of the 3A proteins of enteroviruses

EV-E1, EV-F1, and EV-G1 N-terminally fused to a GB1 solubility tag in *E. coli*. After cleavage of the GB1 tag, the 3A proteins were poorly soluble and tended to aggregate and precipitate at the required concentrations. Therefore, for determination of the dissociation constants of the studied complexes, GB1-fused 3A proteins were used. The strength of the interaction between the recombinant GB1-fused cytoplasmic domains of the 3A proteins and the EGFP-fused GOLD domains of the bovine and porcine ACBD3 proteins *in vitro* was determined by microscale thermophoresis (MST). The MST measurements revealed dissociation constants in the submicromolar range with $K_D = 0.38 \pm 0.03 \mu\text{M}$ for the 3A protein of bovine enterovirus EV-E1 (Fig. 1a), $K_D = 0.68 \pm 0.03 \mu\text{M}$ for the 3A protein of bovine enterovirus EV-F1 (Fig. 1b), and $K_D = 0.17 \pm 0.05 \mu\text{M}$ for the 3A protein of porcine enterovirus EV-G1 (Fig. 1c).

In summary, our data document that the cytoplasmic domains of the 3A proteins of the studied bovine and porcine enteroviruses interact directly with the GOLD domains of the host ACBD3 proteins with dissociation constants approximately 10 times lower than the previously studied 3A proteins of bovine and porcine kobuviruses [19].

Crystal structures of the host ACBD3 GOLD domains in complex with the 3A proteins of selected bovine and porcine enteroviruses and kobuviruses

In our previous studies [19, 20], we determined the crystal structures of complexes composed of the host ACBD3 GOLD domains and the 3A proteins of representative strains of the human enteroviruses EV-A, -B, -C, and -D, the human kobuvirus AiV-A, and the bovine kobuvirus AiV-B. In this study, we extended our previous work to bovine and porcine enteroviruses and porcine kobuvirus. For structural characterization of the 3A proteins of these viruses in complex with the host bovine and porcine ACBD3 GOLD domains (*Bt* GOLD and *Ss* GOLD, respectively), we selected 3A proteins of four viruses, each representing different species as

follows: bovine enteroviruses EV-E1 and EV-F1, porcine enterovirus EV-G1, and porcine kobuvirus AiV-C. The GB1-fused cytoplasmic domains of these 3A proteins were directly co-expressed with the host ACBD3 GOLD domains in bacteria, whole GOLD/3A complexes were purified, and the GB1 tag was removed as detailed in Materials and methods. The recombinant GOLD/3A complexes exhibited properties suitable for subsequent crystallographic analysis.

Of the four studied complexes, we obtained diffraction-quality crystals only for the *Ss* GOLD/AiV-C 3A and *Ss* GOLD/EV-G1 3A complexes (Fig. 2a and c, Table 1). The *Ss* GOLD/AiV-C 3A crystals diffracted to 2.42 Å resolution and belonged to the trigonal P3₁21 space group with one GOLD/3A complex per asymmetric unit, while the *Ss* GOLD/EV-G1 3A crystals diffracted to 2.85 Å resolution and belonged to the triclinic P1 space group with two GOLD/3A complexes per asymmetric unit. Both structures were subsequently determined by molecular replacement using the previously published structure of the unliganded human ACBD3 GOLD domain as a search model (pdb code 5LZ1). The *Ss* GOLD/AiV-C 3A structure was further refined to $R_{\text{free}} = 26.80\%$ and $R_{\text{work}} = 23.44\%$, while the *Ss* GOLD/EV-G1 3A structure was refined to $R_{\text{free}} = 27.21\%$ and $R_{\text{work}} = 23.13\%$.

The *Bt* GOLD/EV-E1 3A and *Bt* GOLD/EV-F1 3A complexes failed to form diffracting crystals even after extensive optimization. To obtain a crystal structure of a 3A protein of any bovine enterovirus in complex with the host ACBD3 GOLD domain, we included several other strains of the same enterovirus species (such as EV-F2 and EV-F3) to our analysis. In addition, we used a protein-fusion strategy originally developed for crystallization of the 3A protein of human enterovirus EV-A71 [20]. Taking advantage of the proximity of the C-terminus of the ACBD3 GOLD domain and the N-termini of the ordered parts of the enterovirus 3A proteins in all previously determined GOLD/3A structures, we connected the last residue of ACBD3 through short peptide linkers to the

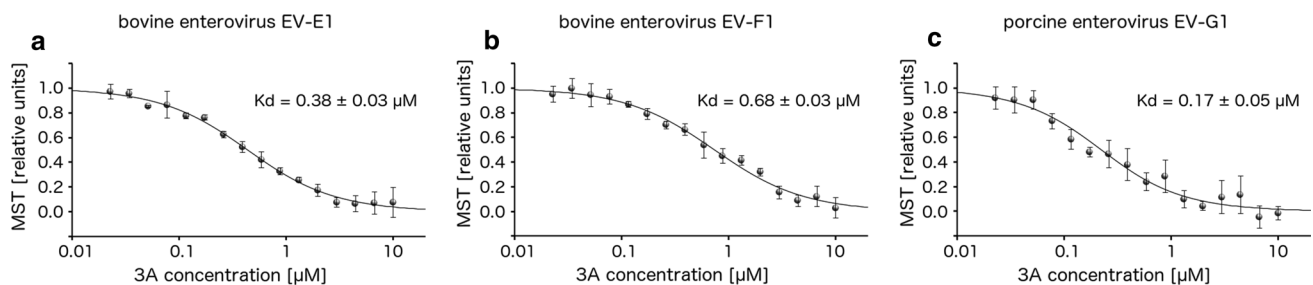


Fig. 1 Biochemical characterization of selected GOLD/3A complexes. **a–c.** Analysis of the interaction of the GB1-fused 3A proteins of bovine enterovirus EV-E1 (**a**), EV-F1 (**b**), and porcine enterovirus EV-G1 (**c**) with the EGFP-fused ACBD3 GOLD domain by micro-

scale thermophoresis. Plotting of the changes in thermophoresis and concomitant fitting curves are shown. Data are presented as mean values \pm standard errors of the mean (SEMs) based on three independent experiments

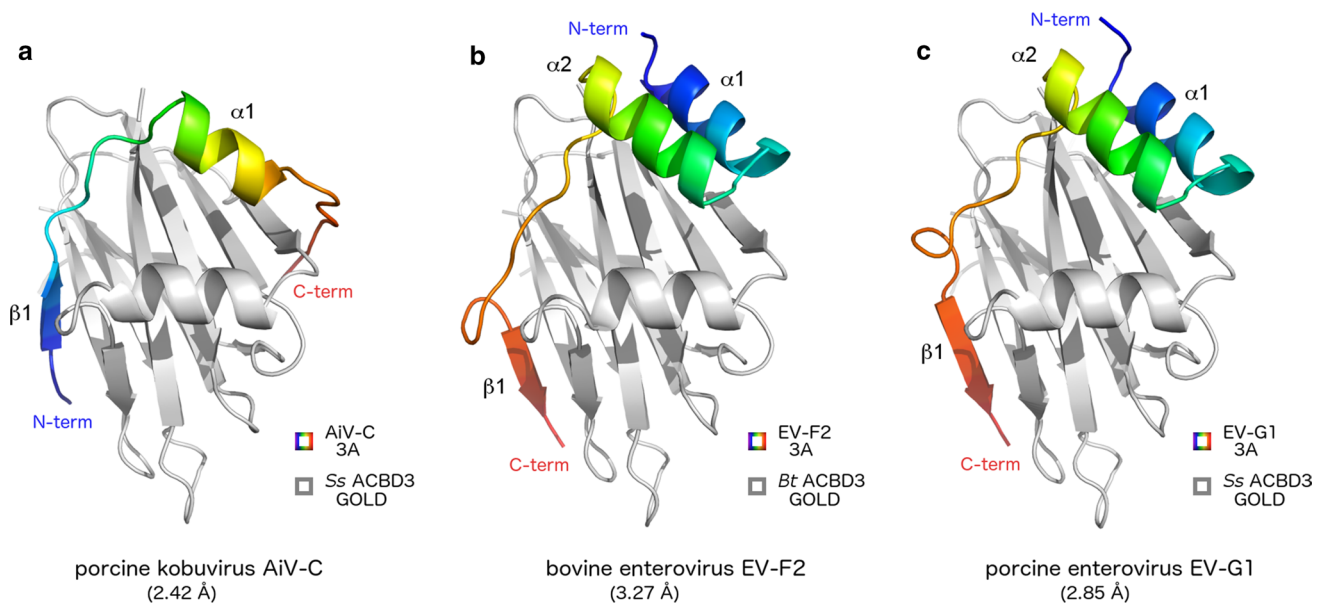


Fig. 2 Structural characterization of selected GOLD/3A complexes. **a-c.** Overall fold of the host ACBD3 GOLD domain in complex with the 3A proteins from porcine kobuvirus AiV-C (**a**), bovine enterovirus EV-F2 (**b**), and porcine enterovirus EV-G1 (**c**). The protein

backbones are shown in cartoon representation. The ACBD3 GOLD domain is depicted in grey, the viral 3A proteins in rainbow colors ranging from blue (N-terminus) to red (C-terminus). *Bt*, *Bos taurus*; *Ss*, *Sus scrofa*

predicted first ordered residues of the studied enterovirus 3A proteins. This approach led to successful crystallization of the *Bt* GOLD/EV-F2 3A fusion protein (Fig. 2b, Table 1). The *Bt* GOLD/EV-F2 3A crystals diffracted to 3.27 Å resolution and belonged to the tetragonal $P4_3$ space group with two GOLD/3A complexes per asymmetric unit. The *Bt* GOLD/EV-F2 3A structure was further refined to $R_{\text{free}} = 27.85\%$ and $R_{\text{work}} = 24.34\%$.

The structure of the *Ss* GOLD/AiV-C 3A complex revealed a high degree of structural similarity to the previously published structures of the *Hs* GOLD/AiV-A 3A and *Bt* GOLD/AiV-B 3A complexes [19] with minor differences in the positions of the central $\alpha 1$ helices of the 3A proteins (Fig. 3a-b). Similarly, the structures of the *Bt* GOLD/EV-F2 3A and *Ss* GOLD/EV-G1 3A complexes revealed a high degree of structural conservation of the GOLD/3A complexes containing the 3A proteins of the human- and livestock-infecting enteroviruses. Minor variations in the conformation of the short linkers between the $\alpha 1$ helices and $\beta 1$ strands of the enterovirus 3A proteins correspond to the lowest primary sequence similarity of these proteins within this region (Fig. 3a and c). Superposition of the crystal structures of the GOLD/3A complexes containing the enterovirus and kobuvirus 3A proteins revealed that the enterovirus and kobuvirus 3A proteins bind to the same regions of the ACBD3 GOLD domain with the opposite orientations of their polypeptide chains (Fig. 3d). Thus, these findings confirmed the previously reported evolutionary convergence [20] in the mechanisms of how enteroviruses and

kobuviruses (regardless of their hosts) recruit ACBD3 to the site of viral replication.

Analysis of the interface between the host ACBD3 GOLD domain and the bovine and porcine enterovirus 3A proteins

In order to identify amino acid residues of the bovine and porcine enterovirus 3A proteins that are involved in the interaction with the host ACBD3 protein, we calculated the changes of the ACBD3-3A interaction energies of various to-alanine mutants of the GOLD/3A complexes using the Pssm tool of the FoldX software package [34] and the atomic coordinates from our crystal structures of the *Bt* GOLD/EV-F2 3A and *Ss* GOLD/EV-G1 3A complexes. These calculations suggested several amino acid residues within several segments of the 3A proteins that are involved in the interaction with the host ACBD3 protein (Fig. 4a). These residues were selected for mutational analysis of enterovirus F2 with to-alanine mutations within the ACBD3-interacting region of the viral 3A protein, specifically for the analysis of the following mutants: L26A/D30A, E32A/R35A, I44A/I49A, and L54A/R56A (Fig. 4a). For all the mutants, the ACBD3-3A interaction was significantly attenuated in the co-immunoprecipitation assay (Fig. 4b), confirming the importance of the selected amino acid residues for this interaction. On the other hand, the interaction with another host factor, GBF1 [35], was preserved in the case of all the mutants except for the L26A/D30A mutant,

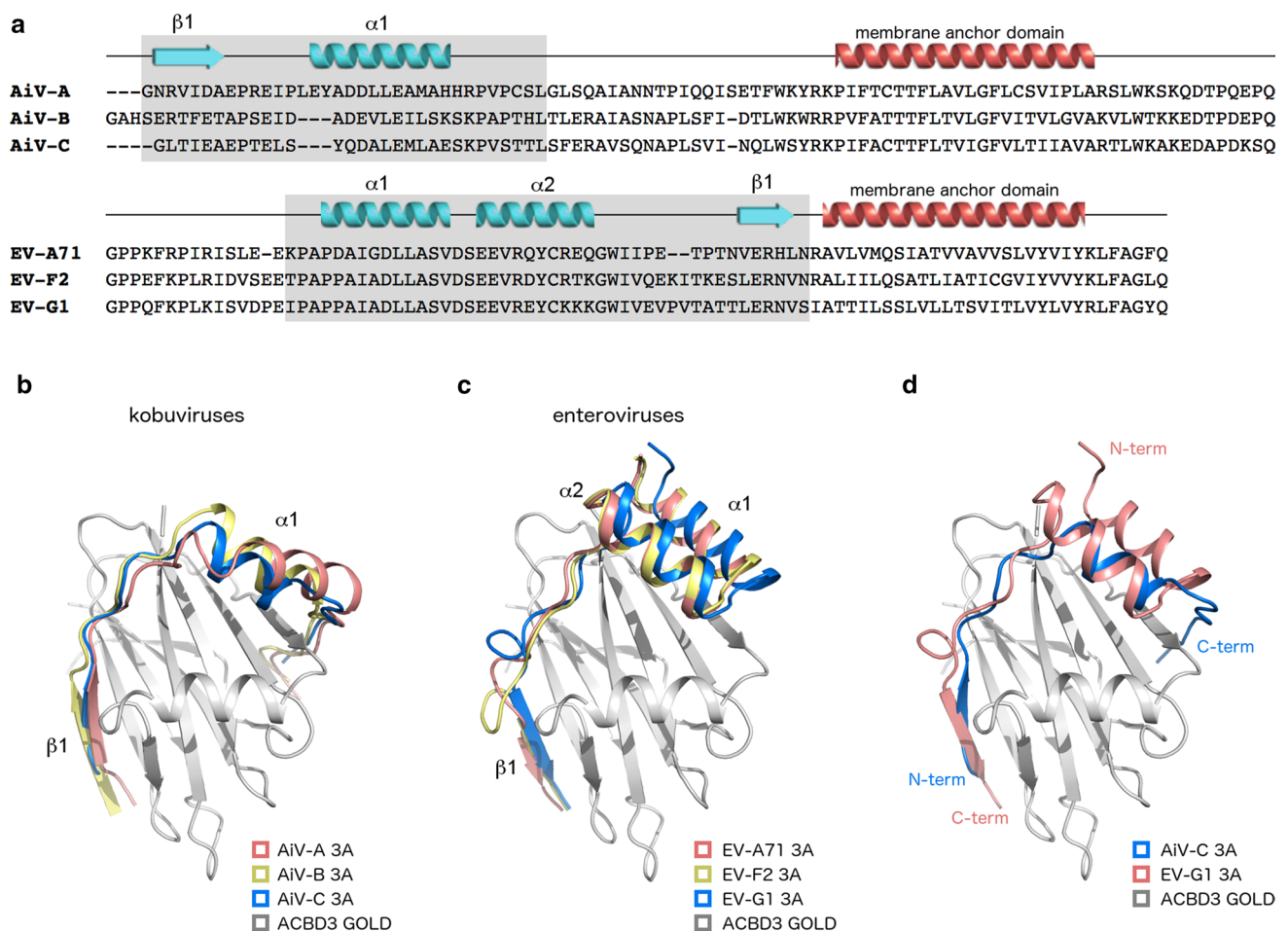


Fig. 3 Convergence in the mechanisms of ACBD3 recruitment by enteroviruses and kobuviruses. **a**. Distinct ACBD3-binding regions of enterovirus and kobuvirus 3A proteins. Sequences of three kobuvirus and three enterovirus 3A proteins are shown. Secondary structures present in the crystal structures of the ACBD3-3A complexes (colored in light blue) and the hydrophobic alpha helices anchoring the 3A proteins to the membrane (colored in red) are indicated above the sequences. ACBD3-binding regions are shaded in grey. AiV-A, human aichivirus; AiV-B, bovine kobuvirus; AiV-C, porcine kobu-

virus; EV-A71, a representative human enterovirus, EV-F2, bovine enterovirus, EV-G1, porcine enterovirus. **b-d**. Superposition of the crystal structures of the ACBD3 GOLD domain in complex with the 3A proteins listed in (a), i.e., kobuvirus 3A proteins (b), representative enterovirus 3A proteins (c), and superposition of the crystal structures of the *Ss* GOLD/AiV-C 3A and *Ss* GOLD/EV-G1 3A complexes (d). The ACBD3 GOLD domain is depicted in grey, and the 3A proteins are colored in red, yellow, and blue as indicated

suggesting distinct, only partially overlapping, binding sites for ACBD3 and GBF1 within the viral 3A protein.

To corroborate the structural data using a biological model and to address the impact of the ACBD3-3A interaction on replication of bovine and porcine enteroviruses, we analyzed replication of both wild-type and mutant enteroviruses using a subgenomic replicon assay reporter. Bovine MDBK and porcine PK-15 cells were transfected with *in vitro*-transcribed viral RNAs of the prototypical strains of the enteroviruses EV-F2 and EV-G1, respectively, with the capsid-protein-encoding regions replaced by the mCherry fluorescent protein-encoding gene, and the reporter mCherry fluorescence was monitored by flow cytometry. Possible background expression of the reporter

directly from the transfected viral RNA was determined using the viral polymerase-lacking mutants ($\Delta 3D^{POL}$). A significant replication of the wild-type replicon RNA was observed in the case of the enterovirus EV-F2 (Fig. 5a-b), but not with EV-G1. Therefore, only enterovirus F2 was selected for further mutational analysis. In the case of all tested mutants of enterovirus F2 with to-alanine mutations within the ACBD3-interacting region of the viral 3A protein (i.e., the L26A/D30A, E32A/R35A, I44A/I49A, and L54A/R56A mutants), the replication rate determined using the reporter subgenomic replicon assay was significantly attenuated (Fig. 5a-b). We observed a mild yet significant effect on the E32A/R35A mutant, a strong effect

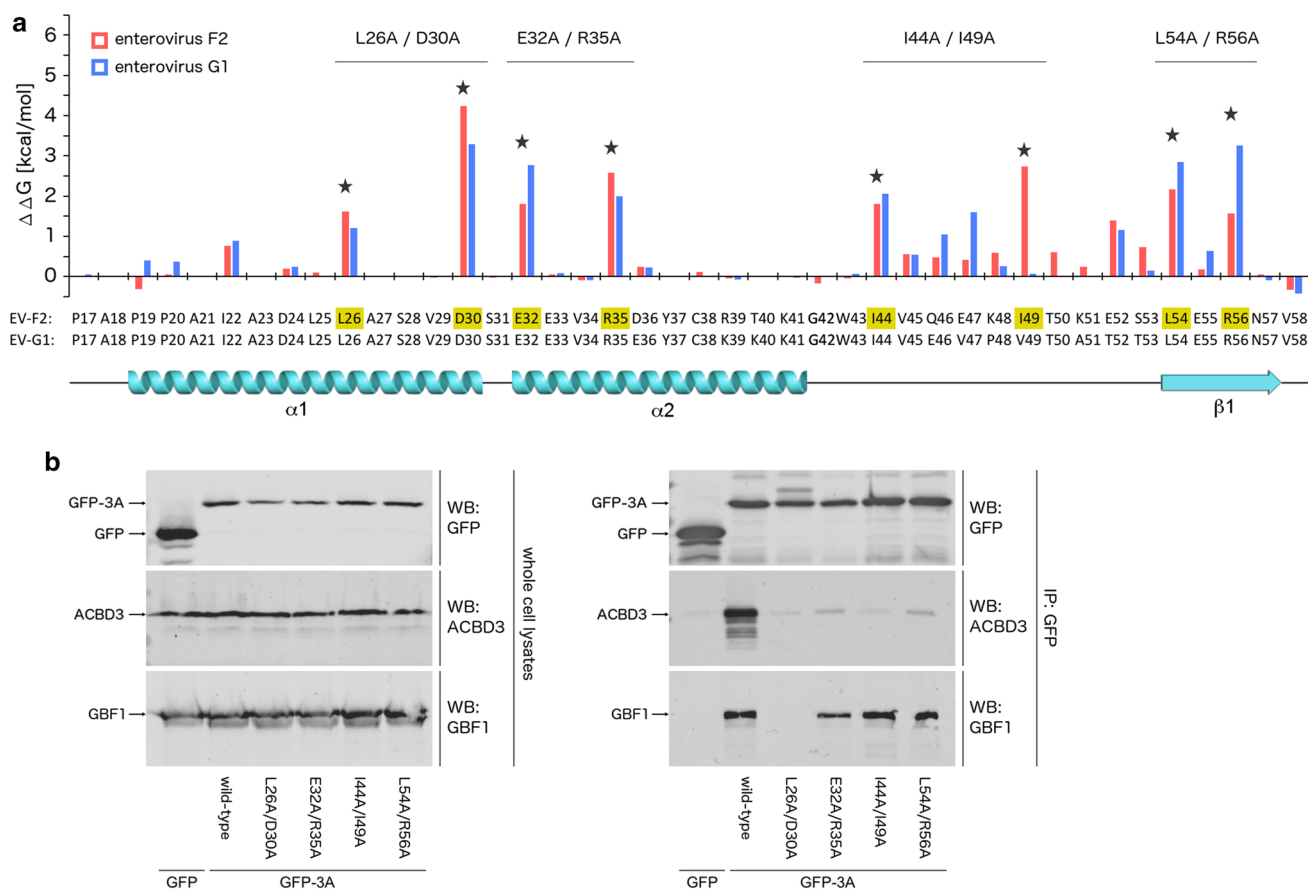


Fig. 4 Design and analysis of the 3A mutants used in this study. **a.** Changes of the ACBD3-3A interaction energies of to-alanine mutants of 3A as obtained with the Pssm tool of the FoldX software package [34] using the crystal structures presented in this work. Amino acid residues used for further design of the 3A mutants are indicated by asterisks. Secondary structures present in the crystal structures of

the ACBD3-3A complexes are indicated under the sequences. **b.** Co-immunoprecipitation of the 3A mutants and endogenous ACBD3 and GBF1. EGFP-fused wild-type 3A of enterovirus F2 and its mutants were overexpressed in HEK293T cells. The 3A complexes were affinity captured by the GFP-Trap nanobody and resolved by immunoblotting as indicated

on the L26A/D30A and I44A/I49A mutants, and no detectable replication of the L54A/R56A mutant.

Taking together, these findings support the conclusion that the interaction between the host ACBD3 protein and the viral 3A protein is required for enterovirus replication.

Discussion

Picornaviruses are small, positive-sense, single-stranded RNA viruses that infect a wide range of mammals, including livestock such as cattle and swine. The picornavirus-mediated livestock infection with the highest impact is bovine foot-and-mouth disease, which is caused by foot-and-mouth disease virus (genus *Aphthovirus*). However, there is increasing evidence of a significant economic impact of livestock infections caused by members of other picornaviral genera, including the genera *Enterovirus* and *Kobuvirus* [2–10]. There are persisting doubts about the virulence

of various strains of these viruses due to the fact that they have been found in both healthy and diseased animals. Nevertheless, serious problems ranging from gastrointestinal and respiratory diseases to abortions potentially caused by some of these viruses can lead to incalculable losses to the livestock farming sector. The vast majority of research on enteroviruses and kobuviruses has been focused on species whose members infect humans, while research on livestock-infecting viruses has been mostly limited to genomic characterization of the viral strains identified.

In this study, we extend our previous knowledge of the non-structural 3A proteins of human-infecting enteroviruses and kobuviruses [19, 20] and present the structural and functional characteristics of the complexes formed by the host ACBD3 protein and the 3A proteins of livestock-infecting viruses. We show that the 3A proteins of the livestock-infecting enteroviruses and kobuviruses bind directly to the host ACBD3 protein. *In vitro*, the dissociation constants of the studied ACBD3-3A complexes were

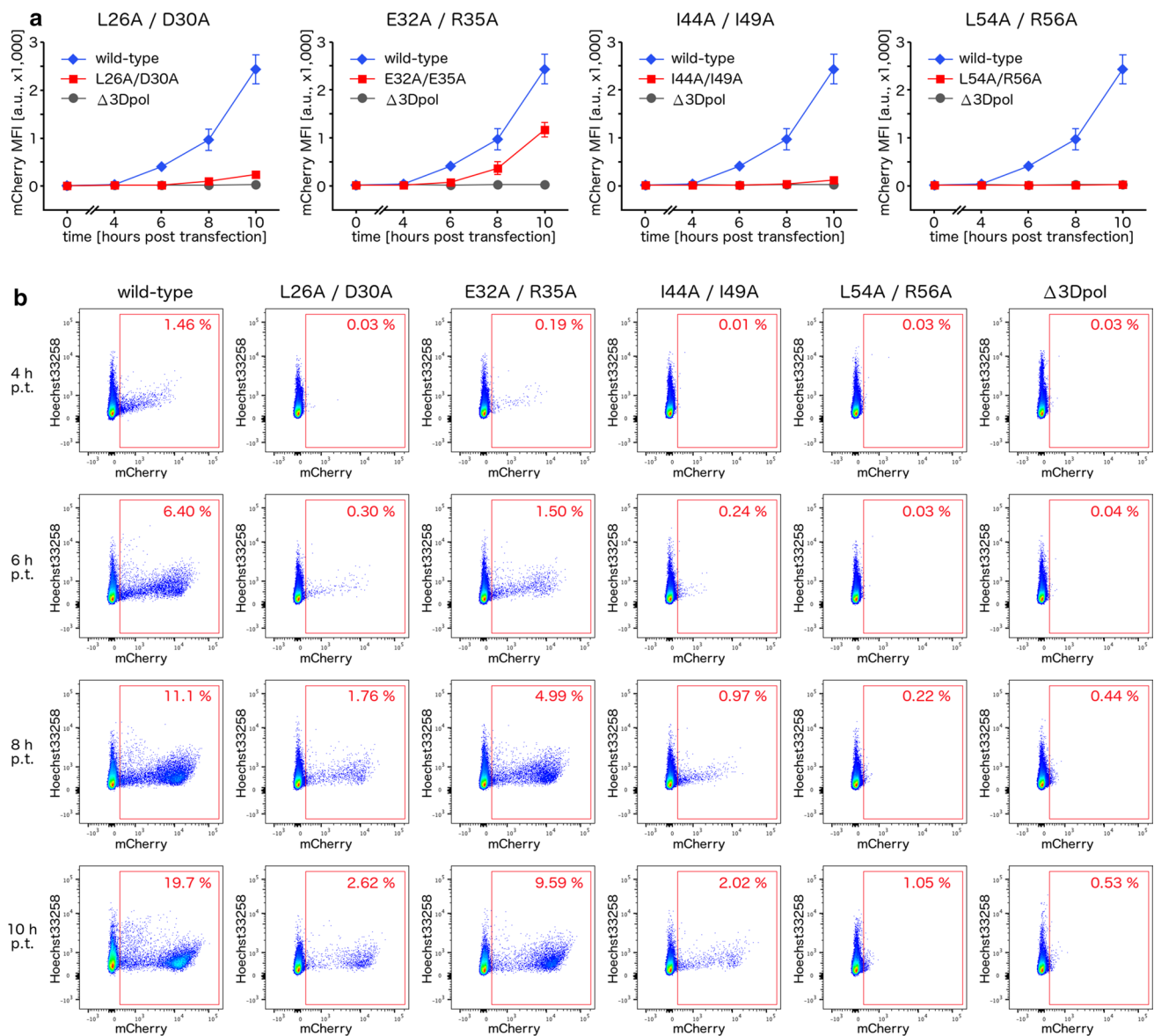


Fig. 5 Analysis of replication of the EV-F2 mutants. **a**. Viral subgenomic replicon assay. Bovine kidney MDBK cells were transfected with the T7-amplified EV-F2 subgenomic wild-type replicon RNA or its mutants, and the mean fluorescence intensity of the reporter mCherry at the indicated time points post-transfection was determined by flow cytometry. A mutant lacking the viral polymerase- ($\Delta 3D^{pol}$) was used as a negative control. The data are presented

as means \pm SEMs from two independent experiments. MFI, mean fluorescence intensity; a.u., arbitrary units. **b**. Raw data of a representative experiment from (a). The percentage of cells with reporter mCherry fluorescence intensity above background is indicated. Staining with Hoechst33258 dye was performed assess cell viability. p.t., post-transfection

lower than those of the previously studied complexes of the human-infecting enteroviruses EV-A to EV-D [20], however, we do not expect this finding to cause any functional consequences *in vivo*, given the fact that even very weak ACBD3-3A interactions can fully support virus replication [20]. Like the 3A proteins of the human-infecting viruses, the enterovirus and kobuvirus 3A proteins, regardless of their host, bind to the same regions of ACBD3 with the opposite polarities of their polypeptide chains

[19, 20]. Although there are some minor variations in the conformations of the linker regions connecting the individual secondary elements of the 3A proteins, the overall architecture of these proteins of the human- and livestock-infecting viruses remains similar. Using structure-guided identification of the amino acid residues involved in the interaction and the viral subgenomic replicon assay with the respective viral mutants, we document the importance of this interaction for facilitation of replication of

the bovine enterovirus EV-F2, as has been observed with human-infecting viruses [20].

The exact role of ACBD3 in enterovirus replication is not yet fully understood, but multiple aspects of ACBD3 recruitment to the site of virus replication should be considered. First, relocation of ACBD3 in virus-infected cells can lead to suppression of the physiological function of ACBD3 (i.e., the regulation of the trafficking pathways between the endoplasmic reticulum and the Golgi), which can limit innate immunity by suppressing the secretion of antiviral cytokines [35] and decreasing MHC-I-dependent antigen presentation of viral peptides [36]. Secondly, viruses may hijack ACBD3 in order to use its physiological abilities for their own purposes and thus redirect the intracellular trafficking towards the sites where the viral genome replication, polyprotein processing, and virion assembly occur. Thirdly, recruitment of ACBD3 to the site of viral replication leads to the recruitment of its interactors and downstream effectors, such as the lipid kinase phosphatidylinositol 4-kinase beta (PI4KB) [12, 13, 17, 18, 37]. Chemical inhibition of PI4KB leads to the arrest of both enterovirus and kobuvirus replication [12, 38], confirming the PI4KB and its product, the PI4P phospholipid, are important host factors of both of these groups of viral pathogens. The elevated concentration of PI4P at the membranes of the viral replication organelles enables the countertransport of PI4P and several other cellular lipids, such as cholesterol and phosphatidylserine, in order to generate membranes with a specific lipid composition suitable for viral replication [39–42]. Mechanistic details of the importance of such a specific and tightly controlled lipid composition of the membranes where viral replication occurs remain to be elucidated.

Accession codes

The crystal structures of the porcine kobuvirus AiV-C 3A protein in complex with the porcine ACBD3 GOLD domain, the bovine enterovirus EV-F2 3A protein in complex with the bovine ACBD3 GOLD domain (fusion protein), and the porcine enterovirus EV-G1 3A protein in complex with the porcine ACBD3 GOLD domain from this publication have been submitted to the Protein Data Bank (<https://www.rcsb.org>) and assigned the identifiers 6Q67, 6Q68, and 6Q69, respectively.

Acknowledgements We are grateful to Carolyn Machamer for sharing the ACBD3-encoding plasmid, and Frank JM van Kuppeveld for fruitful discussions. We thank Helmholtz-Zentrum Berlin for the allocation of synchrotron radiation beamtime. The project was supported by the Czech Science Foundation (Grant number 17-07058Y), Czech Academy of Sciences (RVO: 61388963), and European Regional Development Fund (ERDF/ESF project “Chemical biology for drugging

undruggable targets–ChemBioDrug”, number CZ.02.1.01/0.0/0.0/16_019/0000729).

Author contributions MS performed DNA cloning, protein purifications, and crystallographic experiments, VH contributed to DNA cloning, carried out microscale thermophoresis, the co-immunoprecipitation and viral subgenomic replicon assays, EB conceived the study and revised the manuscript, MK supervised the project, solved the crystal structures, and wrote the manuscript.

References

- Zell R, Delwart E, Gorbalenya AE, Hovi T, King AMQ, Knowles NJ, Lindberg AM, Pallansch MA, Palmenberg AC, Reuter G, Simmonds P, Skern T, Stanway G, Yamashita T, ICTV Report Consortium (2017) ICTV virus taxonomy profile: Picornaviridae. *J Gen Virol* 98(10):2421–2422. <https://doi.org/10.1099/jgv.0.000911>
- Blas-Machado U, Saliki JT, Boileau MJ, Goens SD, Caseltine SL, Duffy JC, Welsh RD (2007) Fatal ulcerative and hemorrhagic typhlocolitis in a pregnant heifer associated with natural bovine enterovirus type-1 infection. *Vet Pathol* 44(1):110–115. <https://doi.org/10.1354/vp.44-1-110>
- Zhu L, Xing Z, Gai X, Li S, San Z, Wang X (2014) Identification of a novel enterovirus E isolates HY12 from cattle with severe respiratory and enteric diseases. *PLoS One* 9(5):e97730. <https://doi.org/10.1371/journal.pone.0097730>
- Candido M, Almeida-Queiroz SR, Buzinaro MG, Livonesi MC, Fernandes AM, Sousa RLM (2019) Detection and molecular characterisation of bovine Enterovirus in Brazil: four decades since the first report. *Epidemiol Infect* 147:e126. <https://doi.org/10.1017/S0950268818003394>
- Yang S, Wang Y, Shen Q, Zhang W, Hua X (2013) Prevalence of porcine enterovirus 9 in pigs in middle and eastern China. *Virology* 453(1):99–109. <https://doi.org/10.1016/j.virus.2013.08.011>
- Knutson TP, Velayudhan BT, Marthaler DG (2017) A porcine enterovirus G associated with enteric disease contains a novel papain-like cysteine protease. *J Gen Virol* 98(6):1305–1310. <https://doi.org/10.1099/jgv.0.000799>
- Bunke J, Receveur K, Oeser AC, Fickenscher H, Zell R, Krumbholz A (2018) High genetic diversity of porcine enterovirus G in Schleswig-Holstein, Germany. *Arch Virol* 163(2):489–493. <https://doi.org/10.1007/s00705-017-3612-x>
- Reuter G, Boros Á, Pankovics P (2011) Kobuviruses—a comprehensive review. *Rev Med Virol* 21:32–41. <https://doi.org/10.1002/rmv.677>
- Reuter G, Nemes C, Boros A, Kapusinszky B, Delwart E, Pankovics P (2013) Porcine kobuvirus in wild boars (*Sus scrofa*). *Arch Virol* 158(1):281–282. <https://doi.org/10.1007/s00705-012-1456-y>
- Park SJ, Kim HK, Moon HJ, Song DS, Rho SM, Han JY, Nguyen VG, Park BK (2010) Molecular detection of porcine kobuviruses in pigs in Korea and their association with diarrhea. *Arch Virol* 155(11):1803–1811. <https://doi.org/10.1007/s00705-010-0774-1>
- Yue X, Qian Y, Gim B, Lee I (2019) Acyl-CoA-binding domain-containing 3 (ACBD3; PAP7; GCP60): a multi-functional membrane domain organizer. *Int J Mol Sci* 20(8). <https://doi.org/10.3390/ijms20082028>
- Greninger AL, Knudsen GM, Betegon M, Burlingame AL, DeRisi JL (2012) The 3A protein from multiple picornaviruses utilizes the golgi adaptor protein ACBD3 to recruit PI4KIIIβ. *J Virol* 86:3605–3616. <https://doi.org/10.1128/JVI.06778-11>

13. Sasaki J, Ishikawa K, Arita M, Taniguchi K (2012) ACBD3-mediated recruitment of PI4KB to picornavirus RNA replication sites. *EMBO J* 31:754–766. <https://doi.org/10.1038/emboj.2011.429>
14. Greninger AL, Knudsen GM, Betegon M, Burlingame AL, DeRisi JL (2013) ACBD3 interaction with TBC1 domain 22 protein is differentially affected by enteroviral and kobuviral 3A protein binding. *mBio* 4:e00098-00013. <https://doi.org/10.1128/mbio.00098-13>
15. Ishikawa-Sasaki K, Sasaki J, Taniguchi K (2014) A complex comprising phosphatidylinositol 4-kinase III β , ACBD3, and Aichi virus proteins enhances phosphatidylinositol 4-phosphate synthesis and is critical for formation of the viral replication complex. *J Virol* 88:6586–6598. <https://doi.org/10.1128/JVI.00208-14>
16. Lei X, Xiao X, Zhang Z, Ma Y, Qi J, Wu C, Xiao Y, Zhou Z, He B, Wang J (2017) The Golgi protein ACBD3 facilitates Enterovirus 71 replication by interacting with 3A. *Sci Rep* 7:44592. <https://doi.org/10.1038/srep44592>
17. Xiao X, Lei X, Zhang Z, Ma Y, Qi J, Wu C, Xiao Y, Li L, He B, Wang J (2017) Enterovirus 3A facilitates viral replication by promoting PI4KB-ACBD3 interaction. *J Virol*. <https://doi.org/10.1128/JVI.00791-17>
18. Lyoo H, van der Schaar HM, Dorobantu CM, Rabouw HH, Strating J, van Kuppeveld FJM (2019) ACBD3 is an essential pan-enterovirus host factor that mediates the interaction between viral 3A protein and cellular protein PI4KB. *mBio* 10(1). <https://doi.org/10.1128/mbio.02742-18>
19. Klima M, Chalupska D, Rozycki B, Humpolickova J, Rezabkova L, Silhan J, Baumlova A, Dubankova A, Boura E (2017) Kobuviral non-structural 3A proteins act as molecular harnesses to hijack the host ACBD3 protein. *Structure* 25(2):219–230. <https://doi.org/10.1016/j.str.2016.11.021>
20. Horova V, Lyoo H, Rózycki B, Chalupska D, Smola M, Humpolickova J, Strating JRP, van Kuppeveld FJM, Boura E, Klima M (2019) Convergent evolution in the mechanisms of ACBD3 recruitment to picornavirus replication sites. *PLoS Pathog* 15(8):e1007962. <https://doi.org/10.1371/journal.ppat.1007962>
21. Shaner NC, Campbell RE, Steinbach PA, Giepmans BN, Palmer AE, Tsien RY (2004) Improved monomeric red, orange and yellow fluorescent proteins derived from *Discosoma* sp. red fluorescent protein. *Nat Biotechnol* 22(12):1567–1572. <https://doi.org/10.1038/nbt1037>
22. Gibson DG, Young L, Chuang RY, Venter JC, Hutchison CA 3rd, Smith HO (2009) Enzymatic assembly of DNA molecules up to several hundred kilobases. *Nat Methods* 6(5):343–345. <https://doi.org/10.1038/nmeth.1318>
23. Hillenkamp F, Peter-Katalinić J (2007) MALDI MS: a practical guide to instrumentation. *Methods Appl*. <https://doi.org/10.1002/9783527610464>
24. Mueller U, Darowski N, Fuchs MR, Förster R, Hellmig M, Paithankar KS, Pühringer S, Steffien M, Zocher G, Weiss MS (2012) Facilities for macromolecular crystallography at the Helmholtz-Zentrum Berlin. *J Synchrotron Radiat* 19:442–449. <https://doi.org/10.1107/S0909049512006395>
25. Kabsch W (2010) XDS. *Acta Crystallogr D* 66:125–132. <https://doi.org/10.1107/S0907444909047337>
26. Krug M, Weiss MS, Heinemann U, Mueller U (2012) XDSAPP: a graphical user interface for the convenient processing of diffraction data using XDS. *J Appl Crystallogr* 45:568–572. <https://doi.org/10.1107/S0021889812011715>
27. McCoy AJ, Grosse-Kunstleve RW, Adams PD, Winn MD, Storoni LC, Read RJ (2007) Phaser crystallographic software. *J Appl Crystallogr* 40:658–674. <https://doi.org/10.1107/S0021889807021206>
28. Adams PD, Afonine PV, Bunkóczi G, Chen VB, Davis IW, Echols N, Headd JJ, Hung L-W, Kapral GJ, Grosse-Kunstleve RW, McCoy AJ, Moriarty NW, Oeffner R, Read RJ, Richardson DC, Richardson JS, Terwilliger TC, Zwart PH (2010) PHENIX: a comprehensive Python-based system for macromolecular structure solution. *Acta Crystallogr D* 66:213–221. <https://doi.org/10.1107/S0907444909052925>
29. Cowtan K (2006) The Buccaneer software for automated model building. 1. Tracing protein chains. *Acta Crystallogr D* 62:1002–1011. <https://doi.org/10.1107/S0907444906022116>
30. Winn MD, Ballard CC, Cowtan KD, Dodson EJ, Emsley P, Evans PR, Keegan RM, Krissinel EB, Leslie AGW, McCoy A, McNicholas SJ, Murshudov GN, Pannu NS, Potterton EA, Powell HR, Read RJ, Vagin A, Wilson KS (2011) Overview of the CCP4 suite and current developments. *Acta Crystallogr D* 67:235–242. <https://doi.org/10.1107/S0907444910045749>
31. Afonine PV, Grosse-Kunstleve RW, Echols N, Headd JJ, Moriarty NW, Mustyakimov M, Terwilliger TC, Urzhumtsev A, Zwart PH, Adams PD (2012) Towards automated crystallographic structure refinement with phenix.refine. *Acta Crystallogr D* 68:352–367. <https://doi.org/10.1107/S0907444912001308>
32. Emsley P, Cowtan K (2004) Coot: model-building tools for molecular graphics. *Acta Crystallogr D* 60:2126–2132. <https://doi.org/10.1107/S0907444904019158>
33. The PyMOL molecular graphics system, Version 1.8 Schrödinger, LLC.
34. Schymkowitz J, Borg J, Stricher F, Nys R, Rousseau F, Serrano L (2005) The FoldX web server: an online force field. *Nucleic Acids Res* 33(Web Server issue):W382–W388. <https://doi.org/10.1093/nar/gki387>
35. Wessels E, Duijsings D, Niu T-K, Neumann S, Oorschot VM, de Lange F, Lanke KHW, Klumperman J, Henke A, Jackson CL, Melchers WJG, van Kuppeveld FJM (2006) A viral protein that blocks Arf1-mediated COP-I assembly by inhibiting the guanine nucleotide exchange factor GBF1. *Dev Cell* 11:191–201. <https://doi.org/10.1016/j.devcel.2006.06.005>
36. Dodd DA, Giddings TH, Kirkegaard K (2001) Poliovirus 3A protein limits interleukin-6 (IL-6), IL-8, and beta interferon secretion during viral infection. *J Virol* 75:8158–8165. <https://doi.org/10.1128/JVI.75.17.8158-8165.2001>
37. Deitz SB, Dodd DA, Cooper S, Parham P, Kirkegaard K (2000) MHC I-dependent antigen presentation is inhibited by poliovirus protein 3A. *Proc Natl Acad Sci USA* 97:13790–13795. <https://doi.org/10.1073/pnas.250483097>
38. Klima M, Tóth DJ, Hexnerova R, Baumlova A, Chalupska D, Tykvar J, Rezabkova L, Sengupta N, Man P, Dubankova A, Humpolickova J, Nencka R, Veverka V, Balla T, Boura E (2016) Structural insights and in vitro reconstitution of membrane targeting and activation of human PI4KB by the ACBD3 protein. *Sci Rep* 6:23641. <https://doi.org/10.1038/srep23641>
39. Mejdrova I, Chalupska D, Plackova P, Mueller C, Sala M, Klima M, Baumlova A, Hrebabecky H, Prochazkova E, Dejmk M, Strunin D, Weber J, Lee G, Matousova M, Mertlikova-Kaiserova H, Ziebuhr J, Birkus G, Boura E, Nencka R (2017) Rational design of novel highly potent and selective phosphatidylinositol 4-Kinase III beta (PI4KB) inhibitors as broad-spectrum antiviral agents and tools for chemical biology. *J Med Chem* 60(1):100–118. <https://doi.org/10.1021/acs.jmedchem.6b01465>
40. Mesmin B, Bigay J, Moser von Filseck J, Lacas-Gervais S, Drin G, Antonny B (2013) A four-step cycle driven by PI(4)P HYDROLYSIS DIRECTS STEROL/PI(4)P exchange by the ER-Golgi Tether OSBP. *Cell* 155:830–843. <https://doi.org/10.1016/j.cell.2013.09.056>
41. Roulin PS, Lötzerich M, Torta F, Tanner LB, van Kuppeveld FJM, Wenk MR, Greber UF (2014) Rhinovirus uses a phosphatidylinositol 4-phosphate/cholesterol counter-current for the formation of replication compartments at the ER-Golgi interface. *Cell Host Microbe* 16:677–690. <https://doi.org/10.1016/j.chom.2014.10.003>

42. Arita M (2014) Phosphatidylinositol-4 kinase III beta and oxysterol-binding protein accumulate unesterified cholesterol on poliovirus-induced membrane structure. *Microbiol Immunol* 58:239–256. <https://doi.org/10.1111/1348-0421.12144>
43. Chung J, Torta F, Masai K, Lucast L, Czapla H, Tanner LB, Narayanaswamy P, Wenk MR, Nakatsu F, De Camilli P (2015) PI4P/phosphatidylserine countertransport at ORP5- and ORP8-mediated ER-plasma membrane contacts. *Science* 349:428–432. <https://doi.org/10.1126/science.aab1370>

Publisher's Note Springer Nature remains neutral with regard to jurisdictional claims in published maps and institutional affiliations.